JOURNAL OF MATERIALS SCIENCE 15 (1980) 2965–2972

Studies of contact damage in polycrystalline zinc sulphide

S. VAN DER ZWAAG, J. T. HAGAN, J. E. FIELD
Physics and Chemistry of Solids, Cavendish Laboratory, Madingley Road, Cambridge, UK

Deformation processes within the grains and grain-boundary sliding are responsible for the formation of the porous zone and the various crack systems around plastic indentations in chemically vapour deposited (CVD) zinc sulphide. The porous zone is formed by gross grain-boundary displacements in the region directly beneath the indenter and all the cracks emanate from around the porous zone and are contained within an extensive plastic zone. For the particular grain orientation used, the material behaves in an ideal elastic/plastic manner with the development of shear flow lines within the porous zone; the interaction of the flow lines with each other or continued slip along the flow lines lead to preferential void nucleation. The porous zone forms at an average representative strain of about 2.5% and a corresponding pressure of 1.5 GPa which is twice the yield stress.

1. Introduction

Recent research on the erosion of brittle solids has been directed towards understanding the role of plastic deformation in producing the crack systems which lead to strength loss and material removal [1–6]. It is known that, in crystals, dislocation interaction can nucleate the crack systems. A related process has recently been identified in soda-lime glasses, where inhomogeneous shear fault lines can develop, interact and nucleate the cracks [5, 7, 8]. The propagation of the cracks is always into the elastic hinterland. In crystalline solids, deformation processes may also be required for the propagation of non-cleavage cracks, such as shear radial cracks in ionic crystals.

In polycrystalline ceramics the nucleation and propagation of the median, radial and lateral cracks around plastic indentations is influenced by the grain size and operating temperatures, both of which can significantly affect the erosion behaviour. Changes in grain size and in temperature can transfer deformation and cracking modes from within the grain itself to events at the grain boundary, such as sliding and voiding, providing deformation modes for both crack nucleation and propagation.

A recent model by Lawn and Evans [9] for the initiation of microfracture beneath sharp indenters assumes the presence of inherent flaws in the bulk. As discussed recently by Hagan [7], it is possible for the deformation processes themselves to produce the necessary defects for crack growth. The assumption of pre-existing cracks is therefore not a necessary one. The present paper gives further evidence in support of the important role which the deformation has in creating the stress field and also the defects for the propagation of the crack systems. This means that theories which consider crack nucleation and propagation in a purely elastic matrix have to be used with caution, especially when considering materials where the propagation of the cracks necessarily requires plastic deformation [10, 11].

Shockey *et al.* [12], Dao *et al.* [13] and Naylor and Page [14] have examined the deformation in polycrystalline zinc sulphide and silicon nitride and in various types of silicon carbide, respectively, by both spherical and Knoop indentations. Naylor and Page observed that the number and extent of lateral cracks around Knoop indentations increased with temperature over the range of ~ 20 to 900° C and attributed this to an increased density of microcracks due to enhanced plasticity at the high temperatures. An observation, hitherto unexplained, which is probably common to most fine-grained brittle polycrystalline solids, is the

0022–2461/80/122965–08$02.80/0

formation of a porous zone directly beneath the plastic indentation in zinc sulphide and silicon nitride [3, 12–14]. Such a porous zone will have a significant effect, not only on the mechanical integrity of the component, but also on its infra-red transparency.

In this paper the deformation and cracking processes around Vickers plastic indentations in chemically vapour deposited (CVD) zinc sulphide will be considered. It will be shown that in quasi-static indentations all the crack systems are contained within the deformed zone; the deformation in this case is by grain-boundary sliding and by slip or twinning within the grains themselves. Directly beneath the indentation, the intergrannular movements are so large as to lead to void formation, both along maximum shear stress trajectories, and also at their intersection points. The porous zone forms at a mean pressure of 1.5 GPa and an average representative strain of about 2.5%. All the crack systems are nucleated along, or at, the intersection points of the flow lines or at the boundary of this porous zone. The crack propagation is intergrannular.

2. Experimental procedure

CVD zinc sulphide with columnar grains in the range of $2\,\mu m \times 2\,\mu m \times 25\,\mu m$ was supplied by Raytheon. The samples were translucent with a milky yellow colour. The average hardness, H, and the critical stress intensity factor, K_{IC}, (measured from Vickers indentations and from the crack system associated with indentations, respectively) were 2.1 GPa and $0.75\,MPa\,m^{1/2}$, respectively. Attempts at sectioning the Vickers impressions by indenting across a pre-existing crack [5, 15] proved unsuccessful because of the roughness of the fracture surfaces. The alternative approach of indenting across the interface (Fig. 1a) of two highly polished blocks held rigidly together in a cold mounting plastic (see Mulhearn [16]) was used instead. The orientation of the columnar grains in the two clamped specimens was such that the longest axis of the grains was normal to the interface between the specimens. The composite specimens were prised apart after indentation to allow examination of the sub-surface damage. Non-interface indentations, such as R in Fig. 1a, were also made on bulk material and they were sectioned by sawing and polishing to allow comparison with interface indentations, such as Q. Both optical and scanning electron microscopy (SEM) were used to examine the surface and sub-surface damage. Spherical indentations at different loads with $800\,\mu m$ diameter tungsten carbide spheres were also made on zinc sulphide

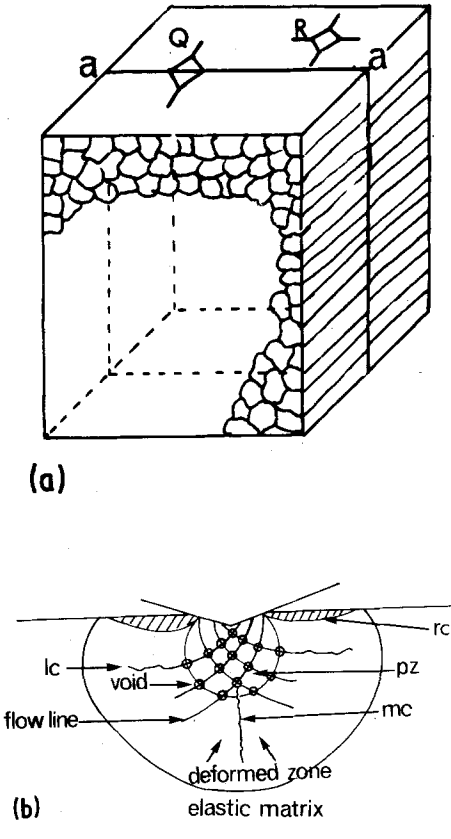

Figure 1 (a) A schematic diagram of the composite block illustrating the grain orientation and the indentations Q and R, respectively, along and away from the bulk interface, aa. (b) A schematic diagram of flow lines in the porous zone, pz, and radial, median and lateral cracks, rc, mc and lc, respectively, within the deformed zone, dz. (c) Plot of the mean contact pressure as a function of the ratio of the contact radius to the sphere radius, a/R. The broken line is the elastic curve.

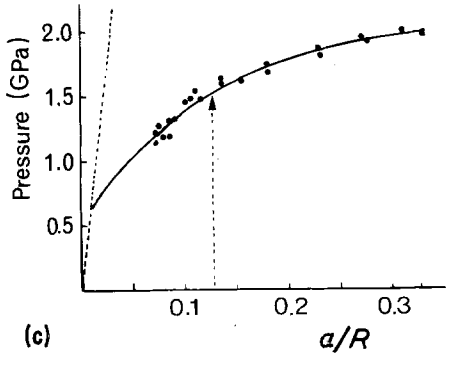

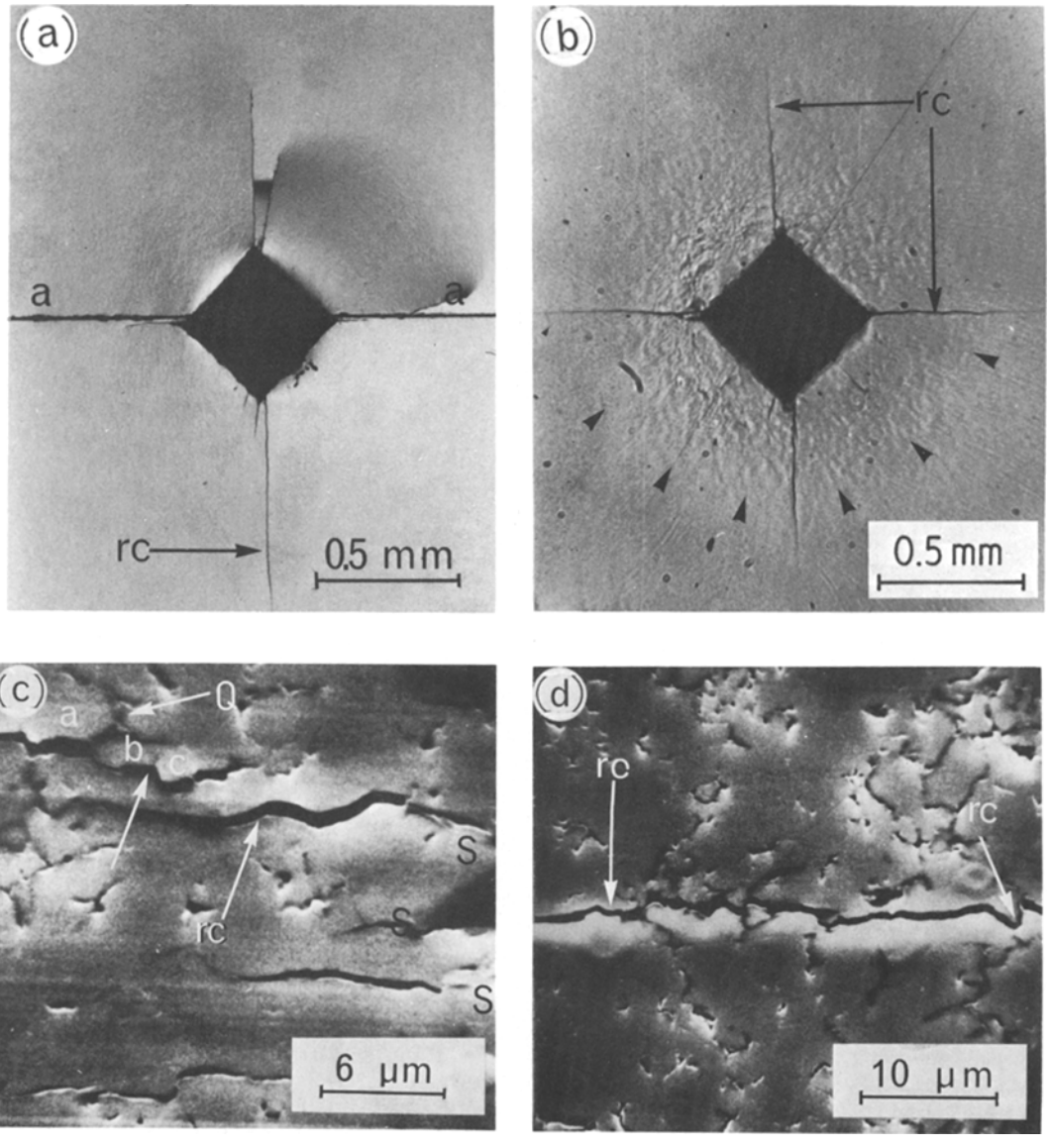

Figure 2 (a) and (b) show the surface damage around interface and bulk indentations; the interface is marked aa. (c) and (d) reveal grains a, b and c being pushed onto the specimen surface and the intergranular nature of the dominant radial crack, rc. Both specimens were lightly etched. (e) Sub-surface damage of an interface indentation revealing a heavily deformed zone, pz, and traces of median and lateral cracks within the plastic zone.

and the residual contact diameter measured. From the measurements it was possible to determine the stress–strain curve (and hence the yield stress) and the corresponding strain for the onset of porosity in the heavily deformed zone directly beneath the indenter. The strain is defined as a constant times the ratio of the contact radius, a, to the ball radius, R.

3. Results

The surface and sub-surface deformation around 300N interface and bulk indentations are compared in Fig. 2. The surface around the indentation is characterized by a dimpled region (clearer and arrowed in Fig. 2b) which marks the size of the plastic zone. The radial cracks, rc, emanate from the corners of the plastic impression and extend as far as the plastic zone. One pair of radial cracks shown in Fig. 2a coincide with the interface, aa, but apart from this the surface damage in the two cases is essentially the same. The dominant deformation mode is grain-boundary slidings, as can be seen in region Q of Fig. 2c, which is an SEM micrograph of a region close to the indentation, sss. Also apparent is the intergranular nature of propagation of the main radial crack, rc. Fig. 2d again reveals the intergranular radial crack propagation. The sub-surface damage of an interface indentation (Fig. 2e) shows traces of lateral cracks and radial and median cracks, (rc and mc respectively) which form at different stages of the loading cycle. The median cracks form first, while the lateral cracks, lc, only develop during the unloading cycle.

All the crack systems emanate from a heavily deformed zone, pz, directly beneath the plastic impression and within the plastic zone. The deformed material surrounding the indentation consists of two zones, namely a spherical zone, pz, whose radius is equal to the diagonal length of the plastic impression and a second larger zone, dz, which extends to the ends of the radial cracks. This second region is the size of the overall plastic zone and the deformation in this case is by grain-boundary sliding and re-orientation in the indentation stress field. Towards the centre of the deformed zone, the intergranular displacements become large enough to lead to void formation and the development of a porouz zone, pz. This is clearly evident in Fig. 3a and b which show transmission optical micrographs of heavily deformed zones around 150N bulk and interface indentations, respectively. The broken arrows mark the size of the porous zone near the specimen surface (the continuous white line). There are traces of median, radial and lateral cracks around the porous zone. The voids in the porous zone scatter the light and therefore appear as black spots. Note that the pore density increases towards the centre of the zone, pz. The voids in the porous zone are shown in greater detail in the SEM micrograph in Fig. 3d which is a higher magnification of a region in Fig. 3c. The voids, V, at the boundaries, are clearly formed by grain-boundary sliding. Away from this porous zone the sliding occurs without any void formation. This grain-boundary sliding is more evident in Fig. 4a which illustrates the displacement of fiducial lines, ff, across the grain boundary. The void formation may require some deformation within the grains themselves. The deformation within the grains is more apparent in Fig. 4b and c which show regions in the subsurface indentations with the loading axis normal to (such as Fig. 1a) and along the axis of the longest axis in the grains a and b. There are also voids along the columns of grains.

Another observation in the porous zone is the development of what appear to be spiral flow lines. Fig. 5a shows the sub-surface damage for a 150N Vickers indentation in which the preferential void formation along the flow lines makes them just discernable. The flow lines are evident for a 300N indentation on a small-grain 0.5 μm × 0.5 μm × 5 μm zinc sulphide specimen, as in Fig. 5b. Median and radial cracks can also be seen in these figures. The width of the distorted zone along the flow lines is influenced by the grain dimensions; the smaller the grain size, the larger and more localized the distortion will be. The flow lines are therefore clearer in the smaller grain material. Higher magnifications of the flow lines in Fig. 5a are arrowed in Fig. 5c and they show the high void density along the flow lines and also the nature of the pores between the grains, as in Fig. 5d. All the featues in the sub-surface deformed zone are illustrated schematically in Fig. 1b.

The stress–strain curve obtained from spherical indentations on zinc sulphide is illustrated in Fig. 1c. The broken line through the origin is the elastic curve. The yield stress, defined as the point of departure from the elastic behaviour, is 0.68 GPa. radius at low pressures (up to 1.2 GPa) and the experimental curve has been extrapolated to the elastic curve. The yield stress, defined as the point

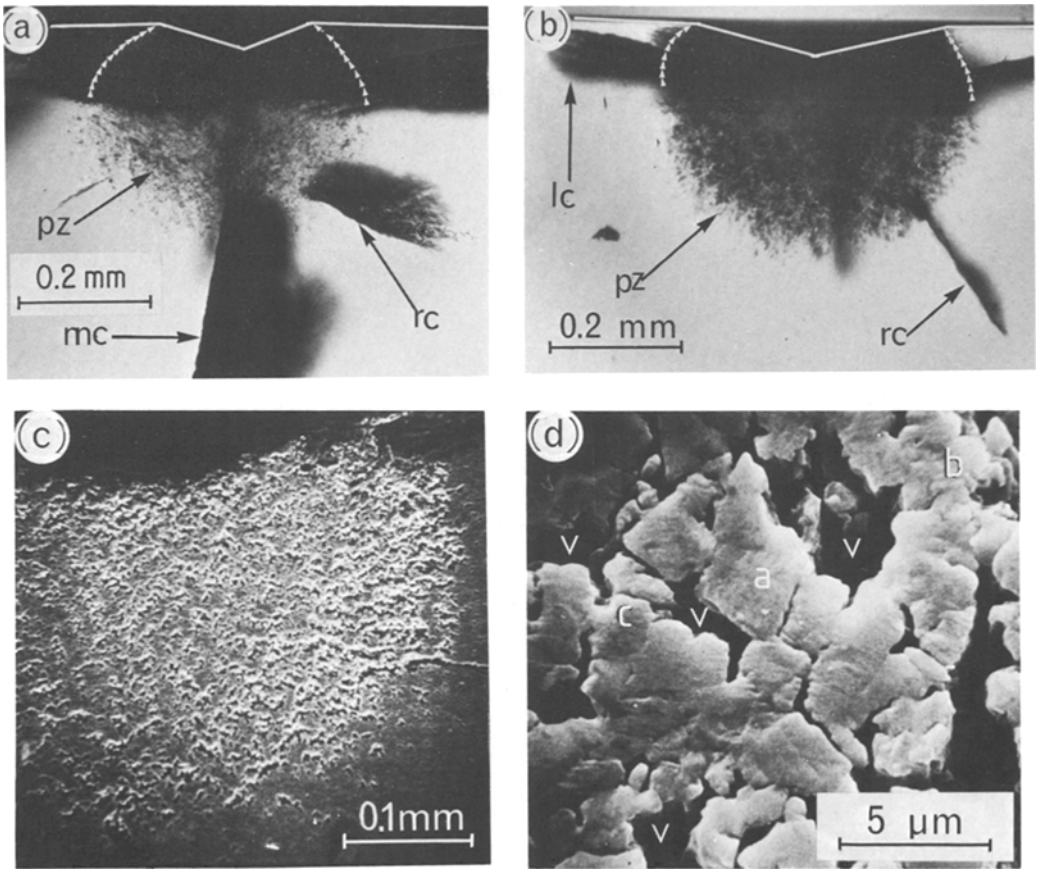

Figure 3 (a) and (b) are transmission optical micrographs of the heavily deformed zones, pz, around 150N interface and bulk indentations, respectively. There are also traces of median, radial and lateral cracks. (c) and (d) are SEM micrographs at different magnifications of regions in (b) and they illustrate the porous nature of the heavily deformed zone, pz.

of departure from the elastic behaviour, is 0.68 GPa. By studying the cross-sections of indentations formed at different loads, the stress and strain at which the porous zone starts to develop have been established as 1.5 GPa and 2.5%, respectively.

4. Discussion

Contact damage in CVD zinc sulphide shows all the characteristic features of indentations in isotropic elastic/plastic solids; namely, the deformed zone and median, radial and lateral cracks. The deformation is accommodated by slip in the grains and grain-boundary sliding which lead to nucleation of voids/crack nuclei and propagation of the various crack systems. Since the deformation process is required for the propagation of the cracks, all the cracks are contained within the plastic zone and do not extend into the elastic hinterland, as occurs, for example, in soda-lime glass.

The most interesting observation within the deformed zone is the existence of a porous region, pz, directly beneath the indenter (see Fig. 3). It has been established very clearly with Fig. 3d that the zone, pz, is made up of voids, formed by the very large displacement of the grains in this region. All the crack systems emanate from around this porous boundary and are nucleated from such voids.

A closer examination of the porous zone has shown the development of shear flow lines which are similar to the inhomogeneous flow lines seen in soda-lime glass [5, 15] amd seen around punch indentations in metals and paraffin (Nadai, [18]). The flow lines follow the maximum shear stress trajectories similar to those which occur around a

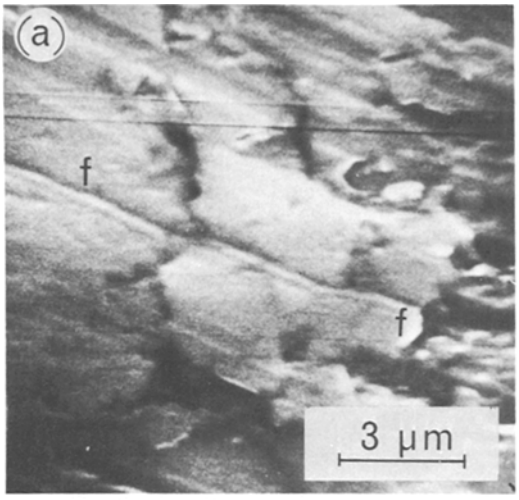

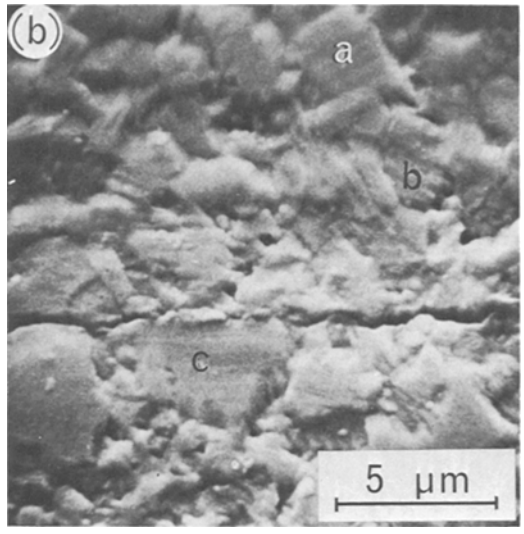

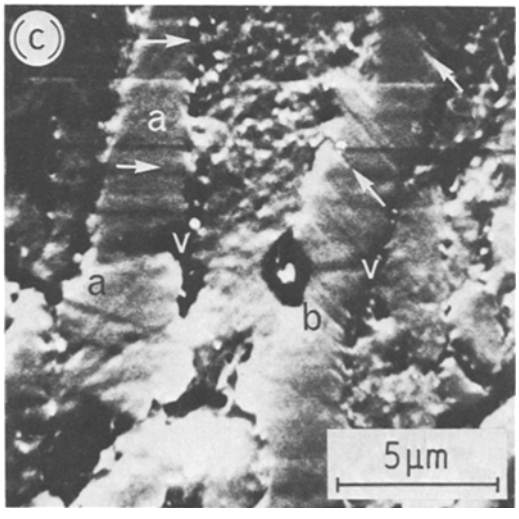

Figure 4 (a) shows the displacements of fiducial line, ff, across the grain boundaries and (b) and (c) show deformation within the grains themselves. The orientation of the grains in (b) is as illustrated in Fig. 1a, while the loading axis in (c) was parallel to the long axis of the grains.

pressurized cylindrical tube in a plastic body. Thus, under quasi-static pyramidal indentations and for the particular orientation of the grains (Fig. 1a), zinc sulphide behaves in an ideally isotropic elastic/plastic manner. The flow lines exist in the whole plastic zone but the preferential pore formation along the flow lines makes them clearer in the porous zone. This high void density along the flow line is clearly visible in Fig. 5c and d. It therefore appears that the flow lines form first and, as the displacements along these build up and the flow lines start intersecting with each other, voids develop along the shear trajectories and at their intersection points. These in turn provide nuclei for the median, radial and lateral cracks as suggested by Hagan and Swain [5] for soda-lime glass.

By the principle of geometric similarity, the mean indentation pressure, P, is given by

$$P = f(a/R), \tag{1}$$

where a/R is the ratio of the contact radius to the indenter radius. For the purely elastic case, this takes the form of

$$P = \frac{8}{3\pi} G_1 \frac{a}{R} [(1-\nu_1) + (1-\nu_2) G_1/G_2]^{-1}, \tag{2}$$

after simplifying Hertz's equation [17] for the relationship between the contact radius, a, and the mean pressure, P. G_1, ν_2 and G_2, ν_2 in Equation 2 are the shear modulus and Poisson ratio for the specimen and indenter materials, respectively.

The dotted line in Fig. 1c is the theoretical curve plotted from Equation 2. The point of departure of the experimental curve from the elastic curve occurs at about 0.68 GPa which is in good agreement with the yield stress, Y, of 0.70 GPa obtained from the Vickers hardness, H, of 2.1 GPa, assuming $H = 3Y$.

Tabor [19] has shown empirically that once the fully plastic stage is reached ($P/Y \simeq 3$), the average representative strain ϵ, in per cent, is given by

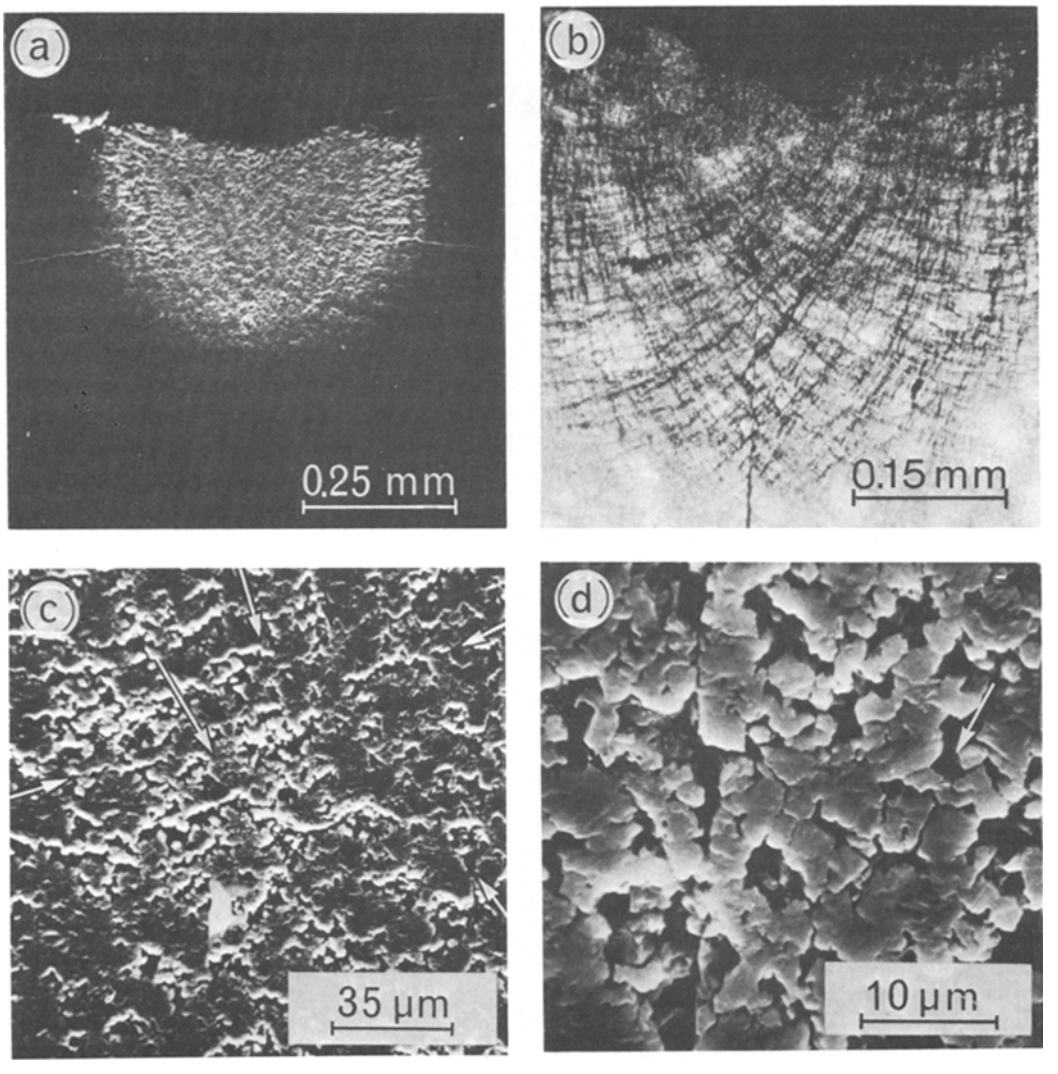

Figure 5 (a) and (b) illustrate the spiral flow lines in the porous zone for the larger and smaller grain size material; (c) and (d) are higher magnifications of (a) and show the high void density along the flow lines.

$$\epsilon = 0.2\left(\frac{a}{R}\right). \tag{3}$$

In Fig. 1c, the above relationship is only applicable to values of $a/R > 0.6$ for which the pressure tends to the Vickers hardness. The strain in the region between the elastic limit and the fully plastic case is not adequately defined by Tabor's relationship. In this paper, however, Equation 3 is used to represent the average representative strain.

Also, from studies of cross-sectional views of these spherical indentations at different loads, it has been established that the porous zone forms at a strain of about 2.5% and is fully developed at a mean pressure of 1.7 GPa which is more than twice the yield stress. This strain value is consistent with the observation that a porous zone is always associated with a Vickers indentation for which there is a constant representative strain of 8% irrespective of the load (Tabor [19]).

5. Conclusion

The observations indicate that during static indentations in CVD zinc sulphide the deformations is accommodated by grain-boundary sliding and by deformation within the grains themselves. The total deformation extends up to the tips of the radial cracks and it is about 2 to 3 times the size of the porous zone from around which all

the cracks emanate. For the particular grain orientation studied, the material behaves in an ideal elastic/plastic manner, with the development of spiral flow lines in the region directly beneath the indenter. As the displacement along the flow lines increases, the grains are sheared past each other, leading to loss of cohesion and void formation. This explains the origin of the porous zone observed under pyramidal indentations in zinc sulphide and silicon nitride [12, 13]. The grain-boundary sliding probably also explains the enhanced lateral cracking in silicon carbide at higher temperatures reported by Naylor and Page [14], since the sliding process will become easier at the higher temperatures and lead to more voids and cracks.

From the erosion and strength degradation point of view, polycrystalline materials provide energy dissipative mechanisms by grain boundary sliding and cracking. An ideal material for this type of contact loading would be one in which appreciable energy dissipation occurs within the grains as well as at their boundaries. It appears that there should exist a critical grain size for which this is possible.

A problem that has to be considered seriously is the effect of the porous zone on the infra-red transparency even in the absence of any strength degrading cracks. This is important especially in situations where the transparency is a critical factor in design.

These studies, together with previous work on soda-lime glass and ionic crystals, have revealed two different types of material response to static indentation with sharp indenters. In the first the deformation process is required for the crack nucleation only, and the subsequent crack propagation is into the elastic hinterland. In the second, the plastic deformation is necessary for both the nucleation and propagation of the various cracks so that all the crack systems are contained within, and limted by, the plastic zone. The zinc sulphide studied in this work fell into the latter category.

Acknowledgements

This work was supported in part by the Ministry of Defence (Procurement Executive) and by the US Air Office of Scientific Research, Grant No. 78-3705.

References

1. B. R. LAWN and M. V. SWAIN, *J. Mater. Sci.* **10** (1975) 113.
2. M. V. SWAIN and J. T. HAGAN, *J. Phys. D: Appl. Phys.* **9** (1976) 2201.
3. A. G. EVANS and T. R. WILSHAW, *Acta. Met.* **24** (1976) 939.
4. I. M. OGILVY, C. M. PERROTT and J. W. SUITER, *Wear* **43** (1977) 239.
5. J. T. HAGAN and M. V. SWAIN, *J. Phys. D: Appl. Phys.* **11** (1978) 2091.
6. A. G. EVANS, M. E. GUILDEN and M. E. ROSENBLATT, *Proc. Roy. Soc.* **A361** (1978) 343.
7. J. T. HAGAN, *J. Mater. Sci.* **14** (1979) 2975.
8. J. T. HAGAN, *J. Mater. Sci.* **15** (1980) 1417.
9. B. R. LAWN and A. G. EVANS, *ibid.* **12** (1977) 2975.
10. J. LANKFORD and D. L. DAVIDSON, *ibid.* **14** (1979) 1662.
11. *Idem, ibid.* **14** (1979) 1669.
12. D. A. SHOCKEY, K. C. DAO and D. R. CURRAN, SRI Report PYU – 4928, Annual Report III, April 1979 (SRI, Menlo Park, California, 1979).
13. K. C. DAO, D. A. SHOCKEY, L. SEAMAN, D. R. CURRAN and D. J. ROWCKIFF, SRI Project PYU – 4928, Annual Report III, May 1979 (SRI, Menlo Park, California, 1979).
14. A. NAYLOR and T. PAGE, Proceedings of the 5th International Conference on Erosion by Solid and Liquid Impact (ELSI V), Cavendish Laboratory, Cambridge, 1979.
15. K. W. PETER, *J. Non. Cryst. Sol.* **5** (1970) 103.
16. T. O. MULHEARN, *J. Mech. Phys. Sol.* **7** (1959) 85.
17. H. HERTZ, "Hertz's Miscellaneous Papers" (Macmillan, London, 1896) Ch. 5.
18. A. NADAI, "Plasticity" (McGraw-Hill, New York, 1931).
19. D. TABOR, "Hardness of Metals" (Clarendon Press, Oxford, 1951) p. 73.

Received 20 March and accepted 29 April 1980.